

Study on point bar residual oil distribution based on dense well pattern in Sazhong area

Based on the dense well pattern data of PI2a unit of Putaohua oil layer in Sazhong development area of Daqing oilfield as well as modern sediment and outcrop, the paper attempts to determine point bar configuration parameters through a combination of quantitative methods to establish a three-dimensional point bar configuration model. On the basis of this model, the paper proposed a parameter-constrained three-dimensional configuration model of lateral accretion interbeds via spatial translation according to the planar trajectory of interbeds, so as to maximally restore the geological structure and ascertain the anisotropism and residual oil inside point bars. The results show that there are 15 interbeds in the study area with an azimuth of 320° and an obliquity range of 3.5° - 13.1° . The interbeds average an interval of 9.5m, and each of them stretches 25m on average. The profile of interbeds is concave, which is slow, steep, slow from the bottom to the top, and the surface takes the shape of crescent. The profile of lateral accretion bodies is characterized by a echelon-like superimposed structure. The interior of point bars shows strong anisotropism due to interbeds, with residual oil being scarce at the bottom, abundant in the middle and extremely abundant at the top. Given the distribution pattern, the paper put forward suggestions for future residual oil potential tapping.

Keywords: Configuration modelling, anisotropism, configuration model, configuration parameter, point bar.

1. Introduction

There have been mature studies on the reservoir stratum configuration of meandering fluvial facies due to advanced technologies. However, configuration

studies confined to geological strata have yet to realize their fine characterisation and application in three-dimensional space. Besides, many results of configuration studies can hardly be applied in exploitation experiments to the fullest. Therefore, it is an important research direction to maximize the application of configuration study results through the combination of three-dimensional modelling and numerical simulation based on the meticulous analysis on reservoir configuration. The study area in the paper is located in Sazhong development area of Daqing oilfield, with the tectonic position at the central depression. Its major exploitation layers are Saertu and Putaohua. With a full understanding of A.D.Miall's internal architectural element analysis and established domestic inner configuration analysis methods of meandering rivers [1-3], the paper conducted a configuration analysis of PI2a unit of Putaohua oil layer to establish the study area's configuration model. On the basis of the model, the paper proposes a set of methods to quantify architectural elements in three-dimensional modelling, set up a fine point bar configuration model, a facies-based model of the point bar's interior, and analyse the inner anisotropism of the PI2 a unit. The results of the configuration study were applied in geological modelling, deepening the understanding of the inner anisotropism of reservoir strata [4-6] and maximally restoring underground geological conditions. Compared to previous studies that rarely realized quantitative modelling of point bar inner configuration, the study made a breakthrough in reservoir stratum modelling by simulating underground geological environment based on static data and accurately describing the oilfield exploitation process. It will better guide future residual oil potential tapping [7-9] by offering reliable theoretical, technical and statistical support.

2. Planar distribution of sand bodies

The PI2 a single layer is mainly consisted of fluvial sediments, with highly developed abandoned channel and point bars as well as severely superposed channel inside the layer. Besides, due to the channel's movement and migration, there are argillaceous or physical interbeds with fine grains and ultra-

Messrs. Shu Yan, Ji Li, Wei He and Shizhong Ma, Northeast Petroleum University, Fazhan Road 99, Daqing 163 000, Shu Yan, The Personnel Development of Daqing Oilfield, Aiguo Road 33, Daqing 163 000, Jianhua Yao, Daqing Oilfield Sanwei Engineering Inspection Co.Ltd., Yinhu Road 3, Daqing 163 000, Xu Zhu, No.1 Oil Production Company, Daqing Oilfield Co. Ltd., Zhongqi Road 34, Daqing 163 000 and Chao Wang, No.2 Oil Production Company, Daqing Oilfield Co. Ltd., Qiangxi Road 15, Daqing 163 000, China. E-mail: luantian1986@163.com

low porosity and permeability, leading to the under-performance of water flooding, leaving part of the oil layer untapped and causing the accumulation of residual oil.

After analysing the profile map of the PI2 a sedimentary unit, the paper found that point bars were scattered on the two sides of the abandoned channel in the bead-like shape, so the point bars could be determined via the abandoned channel. The bottom of the abandoned channel profile was characterised by high gamma, high potential and high resistivity and the top with low gamma, low potential and low resistivity[10]. The point bar profile took on a distinctive dual structure. The erosion surface is characteristic of positive rhythm, with corresponding curves mainly in the shape of box and bell, and features high gamma, high potential and high resistivity [11-12]. The point bar planar distribution pattern was determined after the boundaries of point bars were identified through the abandoned channel and the planar distribution of point bars were identified based on their electro-facies characteristics (Fig.1).

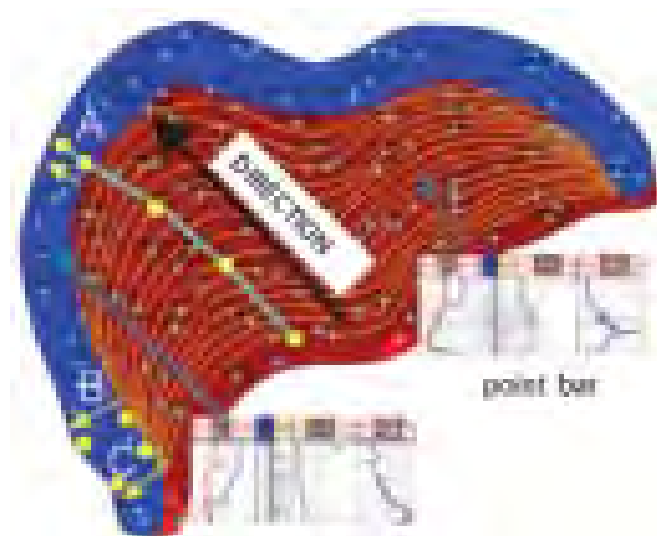


Fig.1 Planar distribution of sedimentary micro-facies and lateral accretion trajectory

3. Point bar configuration profiling

3.1 INCLINATION OF LATERAL ACCRETION INTERBEDS

It is the azimuth of the line connecting the point bar center and the maximal curvature of the abandoned channel, usually pointing to the abandoned channel along its concave bank's normal. The study area has a highly curved abandoned channel, with a sinuosity index of 1.798, plainly indicating the lateral accretion direction of the distributary channel, so the azimuth is 320°

3.2 OBLIQUITY OF LATERAL ACCRETION INTERBEDS

Existing calculation methods of interbed obliquity include core analysis, abandoned surface profiling, determination of the sub-well interface obliquity and fluvial width-to-depth ratio. The paper adopted the dense well pattern abandoned

surface profiling and the width-to-depth ratio to determine the obliquity of lateral accretion interbeds.

3.2.1 Abandoned surface method

An abandoned surface usually refers to the superface of the last lateral accretions and body before the meandering channel is abandoned. Its occurrence is an indirect instruction to characterizing the occurrence of lateral accretion interbeds inside point bars. When the connected well profile is perpendicular to the abandoned channel, if two or more adjacent wells encounter the abandoned surface at the same time, their connected well profile can be used to determine the occurrence of the abandoned surface as well as instructor indirectly characterise the obliquity of lateral accretion occurrence.

Fig.2 shows three pairs of adjacent wells that encounter the abandoned surface at the same time, namely A (ZD262-SE57 and Z60-7), B (ZD271-SE58 and Z62-7) and C (G136-S345 and Z62-307). Take A for example: ZD262-SE57 and Z60-7 are 50m apart, stretching from Northwest to Southeast near the lateral accretion. The ZD262-SE57 PI2a superface is 901.5m and the abandoned surface is 906.5m, 5m from the superface; the Z60-7PI2a superface is 909m and the abandoned surface is 912m, 3m from the superface. The height difference is 2m. As ZD262-SE57 is located aside the concave bank of the abandoned channel and Z60-7 aside the convex bank, the abandoned surface formed by the two wells' lateral accretions and body surfaces is a straight slope, but the actual abandoned surface is concave, which is slow, steep, slow from the bottom to the top. Particularly, at the convex bank of the abandoned channel, there may be a wide gentle slope outside the abandoned channel. In this case, the obliquity can be figured out by using half of the well distance (about 25m) as the boundary of the abandoned channel: $\alpha = \arctan(\Delta h/D) = \arctan(2/25) \approx 4.574^\circ$ (Fig.2)

3.2.2 Width-to-depth ratio method

The equation to calculate the obliquity of lateral accretion interbed is $\alpha = h/W_L$ (h represents the channel's sand body thickness; W_L represents the width of lateral accretion body). According to the Ethridge Schumm relational expression [13], the maximal W_L is 2/3 of the bankfull width of the channel. The width of the abandoned channel drawn according to PI2a single layer's planar sedimentary micro-facies is about 77m, and the channels and body thickness averages 5m. The obliquity is $\alpha = h/W_L = 5/(77 * 2/3) = 5/51.3 = 0.0975$ (that is 5.59°).

Based on a lot of interbed obliquity calculation experience and research data, the paper concluded that the study area's interbed obliquity ranged from 3.5° to 13.1°, with an average of 5.08°.

3.3 INTERVAL OF LATERAL ACCRETION INTERBEDS

The interval between interbeds can be determined by tangent value of the average lateral accretion thickness and

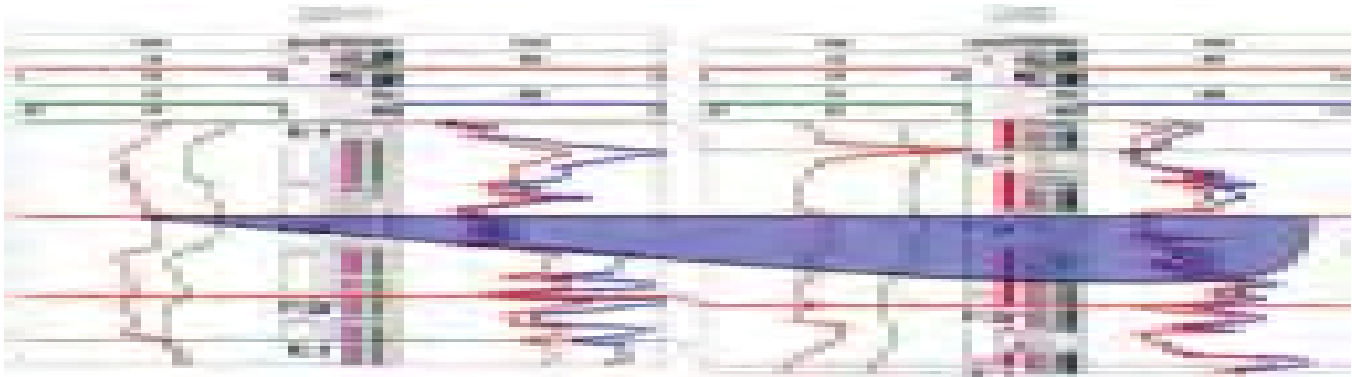


Fig.2 Inter-bed obliquity determined by dense well pattern of abandoned surface (take A for example)

average obliquity. The planar distance is 9.5m, and each interbed stretches about 25m.

3.4 SIZE OF LATERAL ACCRETION BODIES

The size of lateral accretion bodies is mainly calculated by the Ethridge Schumm equation. The abandoned channel is the basis of determining the width and then the size of lateral accretion bodies. The calculation methods of width mainly include the Ethridge Schumm equation, the IGSNRR equation, the Leopold equation and the dense well pattern profiling. The average channel width in the study was 77m. According to the $WL=2W/3$ (WL is the size of lateral accretion bodies; W is the width of the abandoned channel), WL was 51.3m, which meant that the maximal width of lateral accretion surface was 51.3m.

3.5 CONFIGURATION MODELLING

Based on the above study, the paper established a configuration model, with a concave profile that is slow at the top, steep in the middle and slow at the bottom and a crescent surface. The trajectories of lateral accretion intersected data bending point of the meandering curve of the abandoned channel, and the arcs stretched with decreasing curvature and the meandering abandoned channel as the external boundary. Lateral accretion bodies on the profile were echelon-like and superimposed. There were coarses and s with gravels at the bottom of lateral accretion bodies, which reflected scour structure at the bottom of the channel, and different lateral accretion bodies took on different characteristics of sedimentary rhythm (mainly positive rhythm and partly reverse rhythm and composite rhythm). There were a total of 15 lateral accretion interbeds, with an azimuth of 320° and an obliquity range of 3.5° - 13.1° . The interbeds average an interval of 9.5m, and each of them stretches 25m on average (Fig.3).

4. Three-dimensional geological model

In recent years, reservoir stratum configuration modelling has been a hot topic in exquisite modelling technology. Compared to ordinary reservoir stratum modelling technologies, configuration modelling is more able to display the



Fig.3 Configuration model

anisotropism inside reservoir strata and realise modelling on the third, fourth and even smaller-tier inter-faces on the basis of geological statistics. However, due to the complexity of different inter-faces, there are still many problems about configuration modelling, failing to accurately quantify architectural elements or inter-faces in three-dimensional modeling. The paper proposes a method to quantify architectural elements in three-dimensional modelling based on configuration analysis, so as to realise exquisite characterisation of configuration model in three-dimensional modelling and fine representation of reservoir stratum configuration and anisotropism, which can guide future residual oil potential tapping.

4.1 CONFIGURATION MODELLING

An important technology proposed by the paper is to quantify architectural elements, including interbed inclination, interbed obliquity, interbed distance and planar distribution, in three-dimensional modelling. The paper conducted three-dimensional modelling of reservoir strata in side point pars via cooperative constraints of PI2a top and bottom inter-faces and lateral accretion curved surface. As the lateral accretion interbeds are concave, they cannot be calculated by ordinary mathematical algorithms using interpolation. The paper used the azimuth (320°) of P superface's interbed trajectory (Fig.1) along the lateral accretion, with interbed obliquity and target layer thickness as constraints, and spatial translation equations (1), (2), and (3) to complete configuration modelling. Each translation was strictly conducted according to above-mentioned configuration results and eventually the spatial form controlling lateral accretion interbeds was composed (Fig.4).

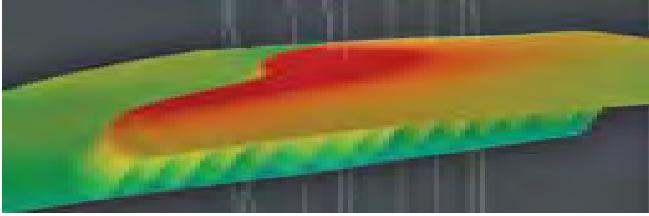


Fig.4 Three-dimensional display of lateral accretion

Spatial translation equations:

$$y_{i+1} = y_i + A \cdot \cos(\theta) \quad \dots \quad (1)$$

$$z_{i+1} = z_i - A \cdot \tan(\varphi) \quad \dots \quad (2)$$

$$x_{i+1} = x_i + A \cdot \sin(\theta) \quad \dots \quad (3)$$

In the equations, x_i , y_i , z_i , x_{i+1} , y_{i+1} , and z_{i+1} represent the point coordinates after the i -th and $i+1$ -th translation of the super face lateral accretion interbed line respectively and “ i ” represents the number of translations; A refers to the planar distance of each translation (unit:m); θ refers to the included angle of lateral accretion direction and due west (unit:degree); φ refers to the interbed obliquity (unit: degree).

4.2 FACIES-BASED MODELLING

Deterministic modelling calculates the cross-well precisely determined reservoir stratum parameter based on existing deterministic materials; stochastic modelling is mainly based on random function theory, during which data of logging, earthquake and core as well as relevant geological knowledge are used to simulate the variation pattern of reservoir strata in corresponding space via stochastic techniques [15]. The paper adopted the sedimentary facies-constrained stochastic modelling [16-17] and opted for the sequential Gaussian algorithm which is suitable to small well spacing and better reflects underground anisotropism. On the basis of configuration and facies model, the porosity and permeability value of the 2/3 part above the interbed was set at 0, so as to resist flow; the 1/3 below the interbed and lateral accretion bodies were analysed by strict variation functions based on their facies types to a certain their major variable range, subordinate variable range and vertical variable range. Eventually, the physical modelling was completed with these sequential Gaussian algorithm.

5. Application

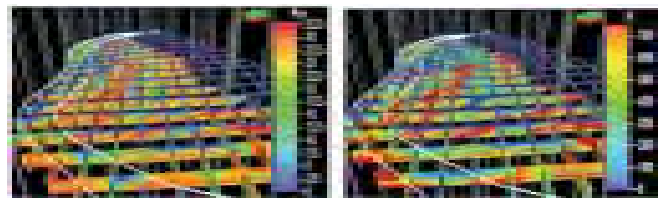
Information about sedimentary model, outcrop and wells scattered across the study area was far enough to depict the anisotropism and residual oil distribution pattern of cross-well reservoir strata. Therefore, the anisotropic variation pattern of cross-well reservoir strata was finely depicted based on the established attribute model; the residual oil distribution pattern was studied with the numerical simulation method.

5.1 STUDY ON ANISOTROPISM INSIDE POINT BAR

Fig.5 shows that reservoir strata inside the point bar featured strong anisotropism and lateral accretion bodies

displayed distinctive positive rhythm, reverse rhythm, and composite rhythm, indicating complex sedimentary environment during the lateral accretion of the meandering channel. The abandoned channel displayed distinctive positive rhythm, reflecting its within-channel sediments at the bottom, medium-fine grained sediments in the middle and overbank sediments at the top; lateral accretion bodies featured varied positive, reverse and composite rhythms, indicating the instability of lateral accretion during the lateral migration of the channel, leading to strong anisotropism and uneven distribution of residual oil inside point bars.

The modelling comprehensively restored the anisotropism of cross-well reservoir strata, displaying its variation pattern. The fence graphic of the study area’s porosity and permeability (Fig.5) shows that the porosity and permeability were located in two areas, including point bar lateral accretion bodies (outside the white frame in Fig.5) and the abandoned channel (inside the white frame in Fig.5). The point bar lateral accretion bodies had good physical properties of medium-high porosity and medium-high permeability (ϕ :15-35%, K :181-1000 $\times 10^{-3} \mu m^2$), but the physical property distribution was not unified in the same lateral accretion body. There were certain lateral accretion bodies with finer sediment particles and bad physical properties, which was related to provenance supply and hydrodynamic force. Besides, there were impermeable interbeds in the top part of lateral accretion bodies to block internal fluids but connected sand bodies with good physical properties at the bottom part; the abandoned channel featured extremely distinctive characteristics, with medium-high porosity and medium-high permeability at the bottom (ϕ : 20-30%, K : 279-860 $\times 10^{-3} \mu m^2$) and extra-low to ultra-low porosity and impermeability to low permeability at the top (ϕ : 0-10%, K : 0-50 $\times 10^{-3} \mu m^2$), representing a typical positive rhythm of abandoned channel. The model's anisotropic parameters included the variation coefficient of permeability at 3.4374, dart coefficient at 77.1426 and anisotropic coefficient at 0.0130, pointing to extremely strong anisotropism caused by the channel's lateral migration, interbeds and sedimentary environment.



A. Porosity model

B. Permeability model

Fig.5 Fence graphic of the study area's at tribute model

Analysis found that lateral accretion interbeds had an very important impact on anisotropism. The study held that interbeds affected the anisotropism of reservoir strata inside point bars in following aspects: (1) dividing thicks and layers into several thin ones; (2) forming impermeable interbeds with adjacent lateral accretion body, impeding injected water

(agent) from reaching oil layers; (3) connected adjacent interbeds tending to cause the partial pinch-out of sand bodies; (4) lateral accretion interbeds with certain porosity and permeability slowing the fluid migration rate to certain extent, impairing the effect of water-flooding.

5.2 STUDY ON RESIDUAL OIL INSIDE POINT BAR

5.2.1 Single well residual oil distribution pattern

Z60-8 and Z60-S307 showed heavily waterlogged characteristics, with a heavily waterlogged bottom, a slightly waterlogged middle and a non-waterlogged top. In point bars, the bottom of wells after long-time water-flooding was heavily waterlogged, with extremely high water saturation and extremely low oil saturation. For instance, the bottom of Z60-8 had a water saturation of up to 63.3% (irreducible water saturation of 17%) while an oil saturation of only 36.7%; its top had a water saturation of 24.7% (irreducible water saturation of 15.8%) and an oil saturation of 75.3%. Besides, water saturation at the bottom of Z60-S307 was up to 65.3% (irreducible water saturation of 17.9%) and oil saturation took up only 34.7%; water saturation at its top was only 23.4% (irreducible water saturation of 14.2%) and oil saturation was as high as 76.6%. It can be seen that in quality reservoir strata, such as point bars, after long-time waterflooding, the bottom of lateral accretion bodies were heavily waterlogged, with ultra-low residual oil content. Meanwhile, the middle and top of the lateral accretion bodies were little affected by waterflooding due to lateral accretion interbeds and thus were slightly waterlogged. Unexploited effective reservoir strata, which still took up a certain proportion, were places where residual oil accumulated and major targets of residual oil exploitation.

5.2.2 Numerical simulation of point bar residual oil distribution pattern

Based on above-mentioned exquisite configuration profiling and results of three-dimensional modelling, the study conducted numerical simulation of point bars in the study area after moderate grid upscaling. The results show that the middle and bottom of point bars were heavily waterlogged, with residual oil saturation ranging from 14% to 28%; the degree of waterlogging at the middle was slighter than that at the bottom, with residual oil saturation of 31%~45%; waterlogging at the top of point bar was the slightest, with highest residual oil saturation of 55%~77.8% (Fig.6). Besides, Fig.6 shows that oil saturation decreased gradually while the degree of waterlogging increased gradually along the inclination of lateral accretion interbeds, which indirectly proved the control of lateral accretion interbeds over residual oil inside point bars. Experiments at physics laboratories have confirmed the point bar residual oil distribution pattern of heavily waterlogged bottom, moderately waterlogged middle and slightly common-waterlogged top due to the existence of lateral accretion interbeds [14].

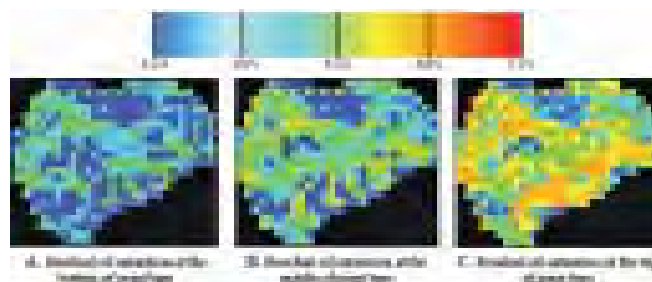


Fig.6 Numerical simulation of residual oil distribution pattern

Therefore, the interior of point bars featured strong anisotropism. The physical properties and the distribution of anisotropism in three-dimensional space were better analysed through the combination of configuration study and three-dimensional modelling, and the adoption of numerical simulation offered a good solution to the exploitation of residual oil in high water-cut oilfields. To improve the exploitation efficiency of residual oil in high water-cut oilfields, deep fracturing or horizontal well fracturing at the top of point bar lateral accretion bodies were recommended to penetrate lateral accretion interbeds, so as to increase the area of oil displacement, improve the efficiency of water injection, enhance the sweep efficiency of injected water and thus water displacement efficiency, according to the characteristics of reservoir strata inside point bars.

6. Conclusion and suggestion

Configuration parameters: There were a total of 15 lateral accretion interbeds, with an azimuth of 320° , an average interbed obliquity of 5.08° , and an obliquity range of 3.5° - 13.1° . The interbeds average an interval of 9.5m, and each of them stretches 25m on average. The average size of lateral accretion body is about 51.33m.

Configuration model establishment: Established a configuration model, with a concave profile that is slow at the top, steep in the middle and slow at the bottom and crescent surface. The trajectories of lateral accretion intersected at a bending point of the meandering curve of the abandoned channel, and the arcs stretched with decreasing curvature and the meandering abandoned channel as the external boundary. Lateral accretion bodies on the profile were echelon-like and superimposed. There were coarses and swith gravels at the bottom of lateral accretion bodies, which reflected scour structure at the bottom of the channel, and different lateral accretion bodies took on different characteristics of sedimentary rhythm (mainly positive rhythm and partly reverse rhythm and composite rhythm).

New configuration modelling method: Proposed a parameter-constrained three-dimensional configuration model of lateral accretion interbeds via spatial translation according to the planar trajectory of lateral accretion interbeds, so as to maximally restore the underground architectural structure.

Achievements and suggestions: Established reservoir stratum attribute model, analysed the impact of configuration (mainly lateral accretion interbeds) on the anisotropism of reservoir strata and concluded that the interior of point bars showed strong anisotropism; found that residual oil was scarce at the bottom, abundant in the middle and extremely abundant at the top; proposed that horizontal wells should be drilled at the top of point bars to penetrate lateral accretion interbeds to increase oil supply units and oil displacement area as a way of residual oil potential tapping.

References

1. Deutsch, C. V. (1992): "Annealing techniques applied to reservoir modelling and the integration of geological and engineering (welltest) data," Stanford University, Vol.306.
2. Srivastava, R. M. (1994): "An Overview of stochastic methods for Reservoir Characterization," In, Yarus and Hamberetal. Stochastic Modelling and Geostatistics: Principles, Methods, and case studies. *AAPG Computer Application in Geology*, Vol.3, pp.3-20.
3. Strebelle, S. and Journel, A.G. (2001): "Reservoir modelling using multiple-point statistics." SPE 71324, 1-11, 2001.
4. Strebelle, S. (2002): "Conditional simulation of complex geological structures using multiple-point-statistics," *Mathematical Geology*, Vol.34, No.1, pp:1-21.
5. Holden, L., Hauge, R., Skare, Ø. and Skorstad, A. (1998): "Modelling of fluvial reservoirs with object models," *Mathematical Geology*, Vol.30, No.5, pp.473-495.
6. Sadeghiazad, M. B. (2017): "Experimental and numerical study on the effect of the convergence angle, injection pressure and injection number on thermal performance of straight vortex tube," *International Journal of Heat and Technology*, Vol.35, No.1, pp.651-656.
7. Fu, T., Liu, J. and Liao, R. (2017): "Water hold up in no-slip oil-water two-phase stratified flow," *International Journal of Heat and Technology*, Vol.35, No.2, pp.306-312.
8. Zeng, F., Tang, J. Sang, Z. and Zhang, H. (2016): "Anexperimental study on the stability bearing capacity of a new type of steel formwork," *Modelling, Measurement and Control B*, Vol.85, No.1, pp.186-197.
9. Zhang, X. P., Sun, J. W. and Sun, Z. C. (2016): "Seismic liquefaction study of sandy soil and its application research." *Modelling, Measurement and Control C*, Vol.77, No.1, pp.65-85.
10. Straka, L.' and Hašová, S. (2016): "The critical failure determination of the constructional parts of autonomous electro-erosion equipment by applying booleanlogic," *Academic Journal of Manufacturing Engineering*, Vol.14, No.2, pp.80-86.
11. Papadopoulos, K., Tzetzis, D., Oancea, G. and Kyratsis, P. (2016): "Reverse engineering of a milk tank and evaluation of volume metering procedure," *Academic Journal of Manufacturing Engineering*, Vol.14, No.1, pp.28-35.

EFFECTIVE UTILIZATION OF GOLD MINERAL RESOURCES BASED ON 3D VISUALIZATION

Continued from page 729

- [19] Zhou L.S. (1998): "Calculation and application of differential-grade gold mines", *Gold Science and Technology*, Vol. 6, No. 4, pp. 45-47.
- [20] Li G.Q., Wang P.Y., Zhao R.K. (2011): "Rock gold mine low-grade resource exploitation practices", *Gold*, Vol. 6, No. 32, pp. 29-33.
- [21] Statsenko L., N.S. Melkounian, (2014): "Modeling Blending Process at Open-Pit Stockyards: A Northern Kazakhstan Mining Company Case Study", *Springer International Publishing*, pp. 1017-1027.
- [22] Wang LG., Song H.Q., Bi L., Chen X. (2017): "Optimization of Open Pit Multielement Ore Blending Based on Goal Programming", *Journal of Northeastern University*, Vol. 38, No. 7, pp. 1031-1036.
- [23] Dobrin C., Bondrea I., Pîrvu B.C. (2015): "Modelling and simulation of collaborative processes in manufacturing", *Academic Journal of Manufacturing Engineering*, Vol.13, No.3, pp.18-25.
- [24] Ferenczi I., Grozav S. (2015): "Modeling the behavior of profinet irt in gigabit ethernet network", *Academic Journal of Manufacturing Engineering*, Vol.13, No.4, pp.13-16.
- [25] Ambethkar V., Kumar M. (2017): "Numerical solutions of 2-D unsteadyincompressible flow with heat transfer in a driven square cavity usingstreamfunction-vorticity formulation", *International Journal of Heat and Technology*, Vol. 35, No.1, pp. 459-473.
- [26] Djedai H., Mdouki R., Mansouri Z., Aouissi M. (2017): "Numerical investigation ofthree-dimensional separation control in an axial compressor cascade", *International Journal of Heat and Technology*, Vol.35, No.1, pp. 657-662.